

INTEGRATED STRATIGRAPHY (RADIOLARIANS AND CALCAREOUS NANNOFOSSILS) OF THE JURASSIC SILICEOUS SEDIMENTS FROM MONTE KUMETA (WESTERN SICILY, ITALY)

MARCO CHIARI¹, ANGELA BALDANZA² & GUIDO PARISI²

Received November 26, 2002; accepted October 23, 2003

Key-words: radiolarians, calcareous nannofossils, integrated biostratigraphy, cherts, Middle-Late Jurassic, Sicily, Italy.

Abstract. Integrated analyses of Calcareous Nannofossils and Radiolarians were carried out in the Monte Kumeta (Sicily) to better define the age of the siliceous sediments (Membro Radiolaritico Intermedio = MRI), which results to be early-middle Bathonian to early Kimmeridgian. The base of this unit shows variable ages in the different sites along the Kumeta palaeoescarpment. Particularly, the ages of the distal sections range from early-middle Bathonian to early Kimmeridgian, whereas the proximal sections show ages from late Oxfordian to early Kimmeridgian. This fact suggests the presence of heteropy between the Membro Radiolaritico Intermedio and the Rosso Ammonitico Inferiore. Moreover, several gaps occur in the MRI and they are restricted to late Bathonian - early Callovian and to late Oxfordian, testifying the times of major tectonic activity along the palaeoescarpment.

Riassunto. Lo studio integrato a radiolari e nannofossili calcarei dei sedimenti calcareo-silicei (Membro Radiolaritico Intermedio = MRI) del Monte Kumeta ha permesso di definirne l'estensione cronologica compresa fra il Bathoniano inferiore (medio) e il Kimmeridgiano inferiore. L'ampiezza dell'intervallo stratigrafico risulta tuttavia variabile lungo la paleoscarpata del Monte Kumeta. In particolare nelle sezioni distali l'inizio della sedimentazione silicea è riferibile al Bathoniano inferiore-medio mentre in quelle prossimali all'Oxfordiano superiore e Kimmeridgiano inferiore. Questi dati evidenziano una eteropia fra il Membro Radiolaritico Intermedio e il Rosso Ammonitico Inferiore. La presenza di lacune, riferibili al Bathoniano superiore-Calloviano inferiore e all'Oxfordiano superiore è indicativa di periodi di maggiore attività tettonica lungo la paleoscarpata.

Introduction

The purpose of this study is to report new biostratigraphic data, obtained from radiolarians and calcareous nannofossils, from the "Membro Radiolaritico Intermedio" (MRI) in the Monte Kumeta (Trapanese Domain, western Sicily). The MRI represents an intermedi-

ate unit between the Rosso Ammonitico Inferiore (MRI) and the Rosso Ammonitico Superiore (RAS) (Di Stefano & Mindszenty 2000). These three units together constitute a succession informally named "Rosso Ammonitico" (Abate et al. 1990).

Several papers deal with the reconstruction of the complex Jurassic stratigraphy of the Monte Kumeta succession (Wendt 1963; 1969; Caflich 1966; Mascle 1979; Di Stefano & Mindszenty 2000; Di Stefano et al. 2002a; 2002b; Marino et al. 2002; Mariotti 2002). The studied area represents an excellent example of the complex syn-sedimentary dynamics in a stepped pelagic escarpment adjacent to a Jurassic infrabasinal high, a product of Early Jurassic extensional tectonics (Di Stefano et al. 2002a; Marino et al. 2002).

Despite the low-moderate preservation of radiolarians and calcareous nannofossils in all the examined sections, this integrated biostratigraphic study allowed to determine the age of the temporal extension of the siliceous sediments, emphasizing a wider stratigraphical range compared to that reported in the literature for Western Sicily.

Geological setting

Monte Kumeta is the central part of an east-west trending ridge, 20 km in length, located in the southern part of the Palermo Mountains near the Piana degli Albanesi village (Western Sicily, Fig. 1a).

This ridge belongs to a structural unit of the intermediate zone of the Sicilian-Maghrebian chain. This unit is derived from the Neogene deformation of a section of the African passive margin known as the Trapanese Domain (Catalano & D'Argenio 1982).

1 C.N.R. Istituto di Geoscienze e Georisorse, Sezione di Firenze, Via G. La Pira 4, 50121 Firenze, Italy. E-mail: mchiari@geo.unifi.it

2 Dipartimento di Scienze della Terra, Università degli Studi di Perugia, Piazza Università, 06100 Perugia, Italy. E-mail: abaldanz@unipg.it - gparisi@unipg.it

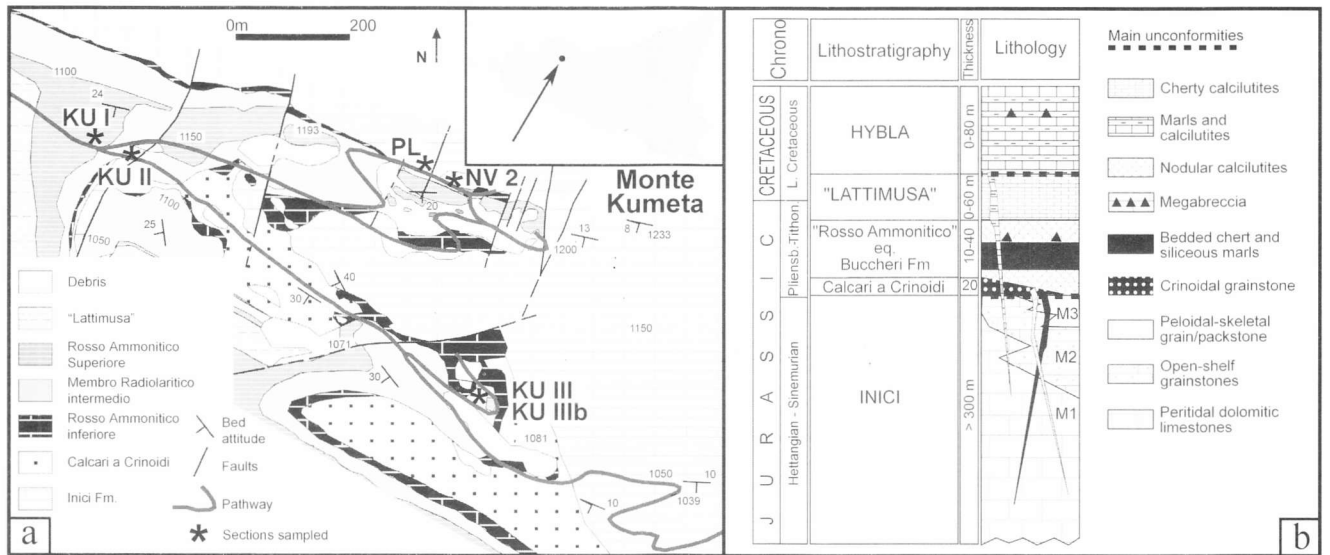


Fig. 1 - a) Geological map of Monte Kumeta with location of the studied sections; b) Lithostratigraphy of Monte Kumeta. (after Di Stefano et al. 2002, modified).

Monte Kumeta represents a Jurassic submarine topographic high which originated in the dissection of larger carbonate platform. It was bounded, to the south, by a basin developed during the late Hettangian-Sinemurian. Di Stefano et al. (2002a) report an accurate reconstruction of the facies architecture in the Jurassic succession of Monte Kumeta coupled with a detailed biostratigraphy aimed to defining the dynamic and genetic factors controlling the conversion of a Bahamian-type carbonate platform to a pelagic escarpment, connecting the Monte Kumeta high to the basin. Progressive northward retreat of this scarp resulted into a gradually steepening slope, along which the distribution of sediments was controlled

mainly by tectonic and gravity induced modifications of the substrate topography.

The Jurassic of Monte Kumeta shows vertical and lateral changes in the geometry of the lithofacies suggesting a depositional environment deeply influenced by re-activation of basinward dipping normal faults.

The existence of stepped surfaces in which the sediments accumulated is evidenced by the relationships of the platform strata (Inici Formation) and the overlying Pliensbachian encrinites. The encrinite bodies show prismatic geometry becoming thicker toward the South and, in some cases, represent the filling of the first generation of neptunian dykes.

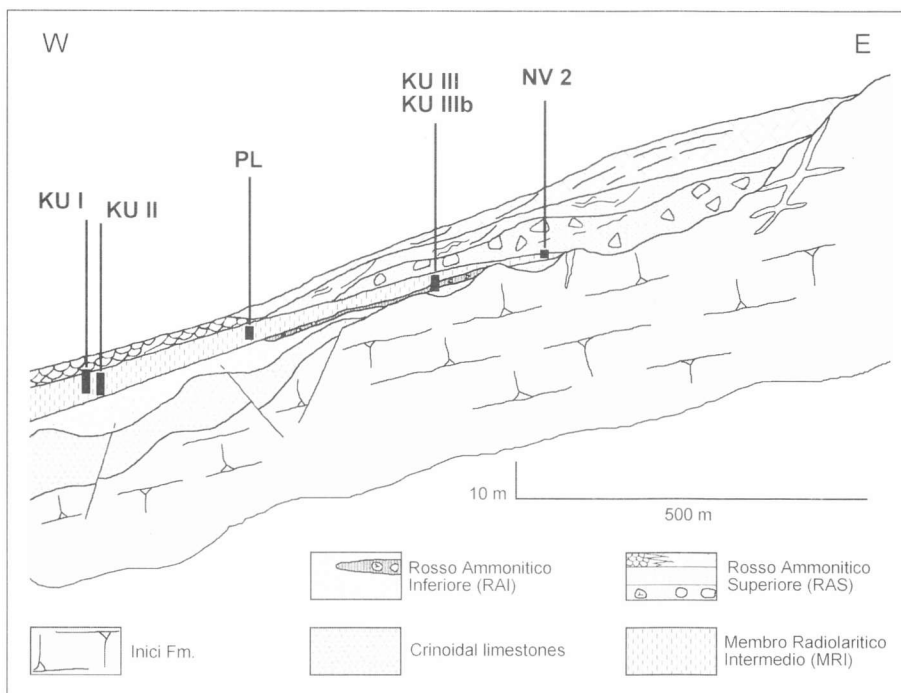


Fig. 2 - Schematic representation of the stratigraphic setting of the Jurassic deposits of Monte Kumeta, as reconstructed along an E-W transect with the studied sections (after Marino et al. 2002, modified).

The encrinite bodies are capped by a thick ferromanganese crust generated, probably by complex changes in water chemistry and related to the “Early Toarcian Anoxic Event” (Di Stefano et al. 2002a). The Fe-Mg crust is dissected by several faults, that created an articulate surface with hollows/depressions in which the pelagic sediments were deposited from the Bajocian to the Oxfordian. The pelagic sediments (Rosso Ammonitico) show clear onlapping relationships with the Crinoidal limestones and the Inici Formation carbonate platform beds (Fig. 1b, Fig. 2). The Lattimusa and the Hybla formations (uppermost Jurassic - Lower Cretaceous), which consists of calcilutite and marls, follow upwards (Fig. 1b).

Lithostratigraphy of the Rosso Ammonitico

The Jurassic Monte Kumeta succession shows evident lateral changes in the geometry of its lithofacies. For this reason it has been necessary to study several sections in the intermediate unit of the Rosso Ammonitico.

The succession, informally named Rosso Ammonitico (Buccheri Formation equivalent), has been subdivided from bottom to top, into three units (Di Stefano & Mindszenty 2000):

Rosso Ammonitico Inferiore (RAI). About 10 m of reddish condensed limestones of Toarcian-middle Oxfordian age (Di Stefano et al. 2002b). The RAI was subdivided into four subunits: 1) RAIa - red limestones with abundant ammonites, fragments of *Bositra*, radiolarians, mollusc fragments and benthic foraminifera (Toarcian-Bajocian); 2) RAIb - pink limestones constituted of alternating laminae of coarser and finer bioclastic grain-pack-wackestone with *Bositra*, foraminifers, ostracods, ammonites, gastropods and echinoderm fragments (upper Bathonian); 3) RAIc - red marly limestones with radiolarians, benthic foraminifera, mollusc and echinoderm fragments (Callovian); 4) RAI d - red, grey, light brown marls, characterized by abundant belemnites, aptychi, corals, crinoids, rhyncholites and echinoderm fragments. Based on belemnites the age of this last subunit is late Callovian - middle Oxfordian (Mariotti 2002).

The RAIb shows a lenticular geometry and the contact with the overlying subunit is discordant and locally marked by a hardground. The contact of RAIc with the overlying red-nodular marls (RAI d) is sharp, marked by a thin discontinuous Mn-oxide crust of middle Callovian age with clear evidence of microbial activity (Di Stefano et al. 2002b).

Membro Radiolaritico Intermedio (MRI). It consists of cherts and cherty limestones, greenish-grey at the base and reddish at the top, and subordinated marls. This unit is clearly wedge-shaped, reaching its maximum thickness (about 10 m) in the southern sector of Monte

Kumeta; the unit pinches out northeastwards, and disappears 200 m from the top of the mountain. Pebbly mudstone intercalations in this unit are well visible near the top of Monte Kumeta.

Rosso Ammonitico Superiore (RAS). It is made of 10-15 m thick, reddish to pink, nodular limestones and *Saccocoma*-limestones, with megabreccia and pebbly mudstone intercalations, of Kimmeridgian - early Tithonian age. This unit exhibits the greatest lithofacies variability. It consists of an apparently heterogeneous complex of breccias, very fine to coarse calcarenites, nodular limestones, and sand-size echinoid skeletal debris. Along the palaeoescarpment these rock types are organised into different sedimentary bodies. Resedimented deposits (mainly megabreccias) predominate in the proximal sector, where they unconformably overlie the RAI sediments, these latter lying in turn unconformably on the Inici Fm. (Fig. 2).

Ammonites provide biochronological constraints for the base of the RAS. The basal breccia yielded *Pseudowaagenia acanthomphala* Herbig of the late Kimmeridgian (Marino et al. 2002). It is worth to note that this ammonite may easily be reworked and thus the age of the breccia could be somewhat younger.

Studied sections

In this study six sections, located in a small area of about 700x300 m have been examined (Fig. 1a).

KU I Section: the section is located along the road running down to the “Cava Cerniglia” (Figs. 1a, 2 and 3a). Here is exposed the upper boundary of the MRI. The thickness of the section is about 3 m. From bottom to top it consists of (Fig. 4): 1) about 5 cm of light brown marls; 2) 2 m of green, grey-green, light brown cherts (layers from few mm to 12-15 cm) and whitish marly limestones (layers of about 1 cm); 3) 80 cm of red cherts (prevalent) and grey-green, light brown cherts (layers of 5-10 cm). Upwards the Rosso Ammonitico Superiore follows, through an irregular surface.

KU II Section: this section is located along the road to “Cava Cerniglia” (Figs. 1a, 2 and 3b) about one hundred metres far from section KU I. The thickness of KU II is about three metres and it consists (Fig. 4), in the lower part, of black and grey cherts (layers from 5 to 20 cm) and, in the upper part, of grey-yellowish cherts (layers from 5 to 10 cm).

PL Section: this section is located in the northern side of Monte Kumeta along the pathway (Figs. 1a, 2 and 3e). The section includes from the bottom to top (Fig. 4): 1) 16 cm of red cherts and 2 cm of dark red clays; 2) about 20 cm of whitish marly limestones, cherty limestones (with red cherts) and light brown marls; 3) 27 cm of cherty limestones (with red cherts at the bottom); 4) 130 cm of pebbly mudstone; 5) 20 cm of light brown

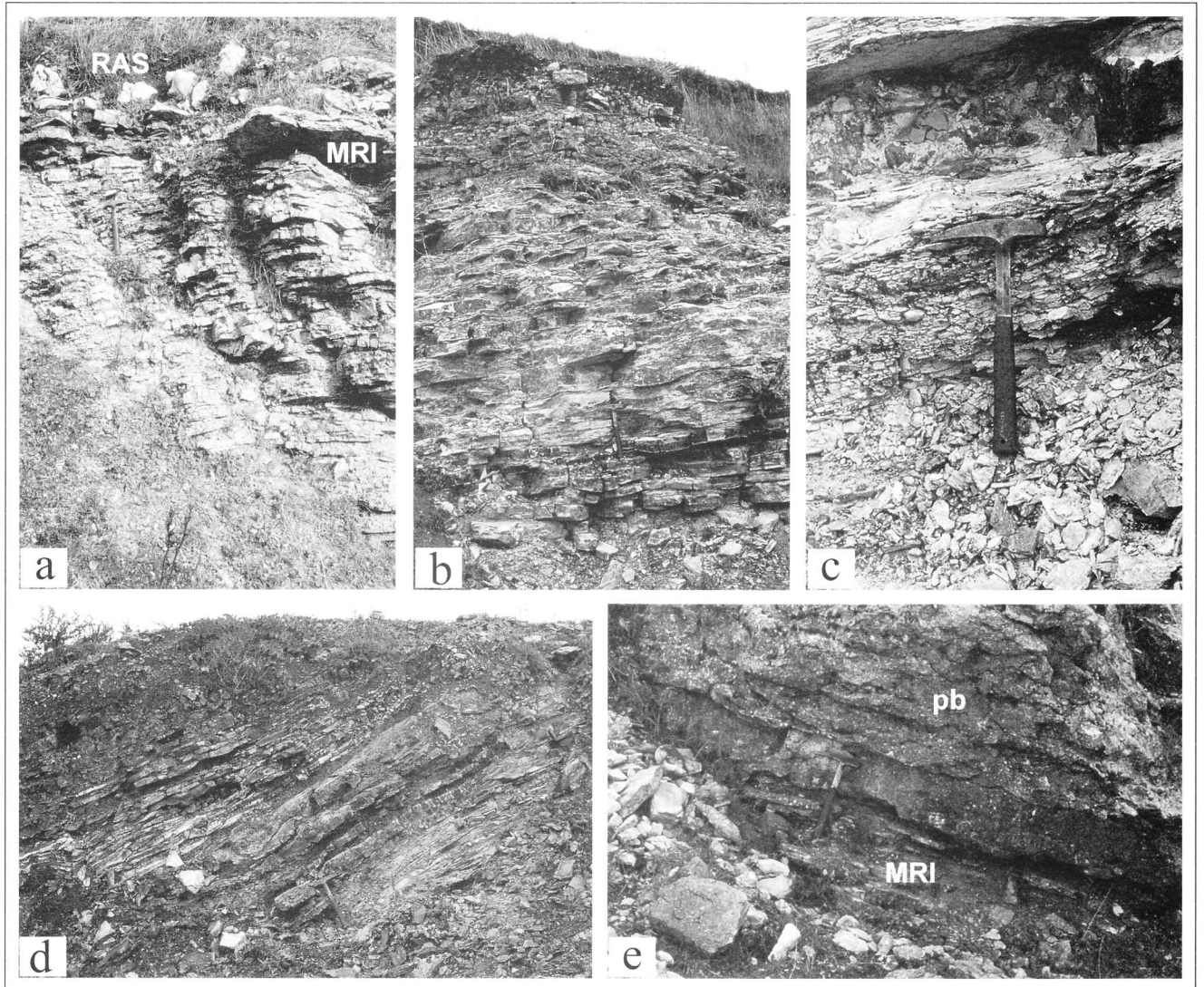


Fig. 3 - Panoramic view of the studied outcrops: a) KU I section, contact between Membro Radiolaritico Intermedio (MRI) and Rosso Ammonitico Superiore (RAS); b) KU II section; c) KU IIIb section, RAId (belemnite level of Rosso Ammonitico Inferiore); d) KU III section; e) PL section, contact between the MRI and pb (a pebbly mudstone lithofacies in the Membro Radiolaritico Intermedio).

marls, pink cherty limestones (with red chert) and red cherts; 6) 21 cm of limestones; 7) another level (30 cm) of pebbly mudstone.

KU III Section: this section is located in the “Cava Cerniglia” (Figs. 1a, 2 and 3d), near the KU IIIb section. Here the lower boundary of the MRI on the RAI is exposed. The thickness of the section is about 1.90 m and it consists from bottom to top of (Fig. 4): 1) hardground of middle Callovian age (Di Stefano et al. 2002b); 2) a few centimetres of belemnite-bearing marls (belonging to the RAI); 3) 33 cm of pink marly limestones (layers of 3-5 cm); 4) 90 cm of pink cherty limestones (with red cherts) and pink and grey marls, the layers of cherty limestones having a variable thickness of 4-10 cm and the cherts have a thickness from 3 to 7 cm; 5) about 20 cm of pink silicified limestones (layers of 2-5 cm) alternating with greenish clays; 6) the top of the section comprises about 50 cm of red bedded cherts (layers of 2-12 cm).

KU IIIb Section: also this section is located in the “Cava Cerniglia” (Figs. 1a, 2 and 3c). Here the lower boundary of the MRI on the RAI is exposed. The section is 2.90 m thick and consists of (Fig. 4): 1) hardground of early Toarcian age (Di Stefano et al. 2002a; 2002b); 2) about 8 cm of pinkish marls (belonging to the RAI); 2) hardground of middle Callovian age (Di Stefano et al. 2002b); 3) about 80 cm of belemnite bearing reddish-light brown marls (belonging to the RAI); 4) 1.05 m whitish-pink cherty limestones (layers from 2 to 15 cm, with whitish and red cherts) and yellowish, green marls (layers of 1-5 cm); 5) 43 cm of whitish cherty limestones (layers from 1 to 5 cm with whitish and red chert); 6) about 51 cm of red-yellowish cherts (layers of 2-7 cm).

NV 2 Section: this section (Figs. 1a, 2) is located in the northern side of Monte Kumeta along the pathway near section PL. Here the upper boundary of the MRI is exposed. The section consists (Fig. 4) of about 80 cm

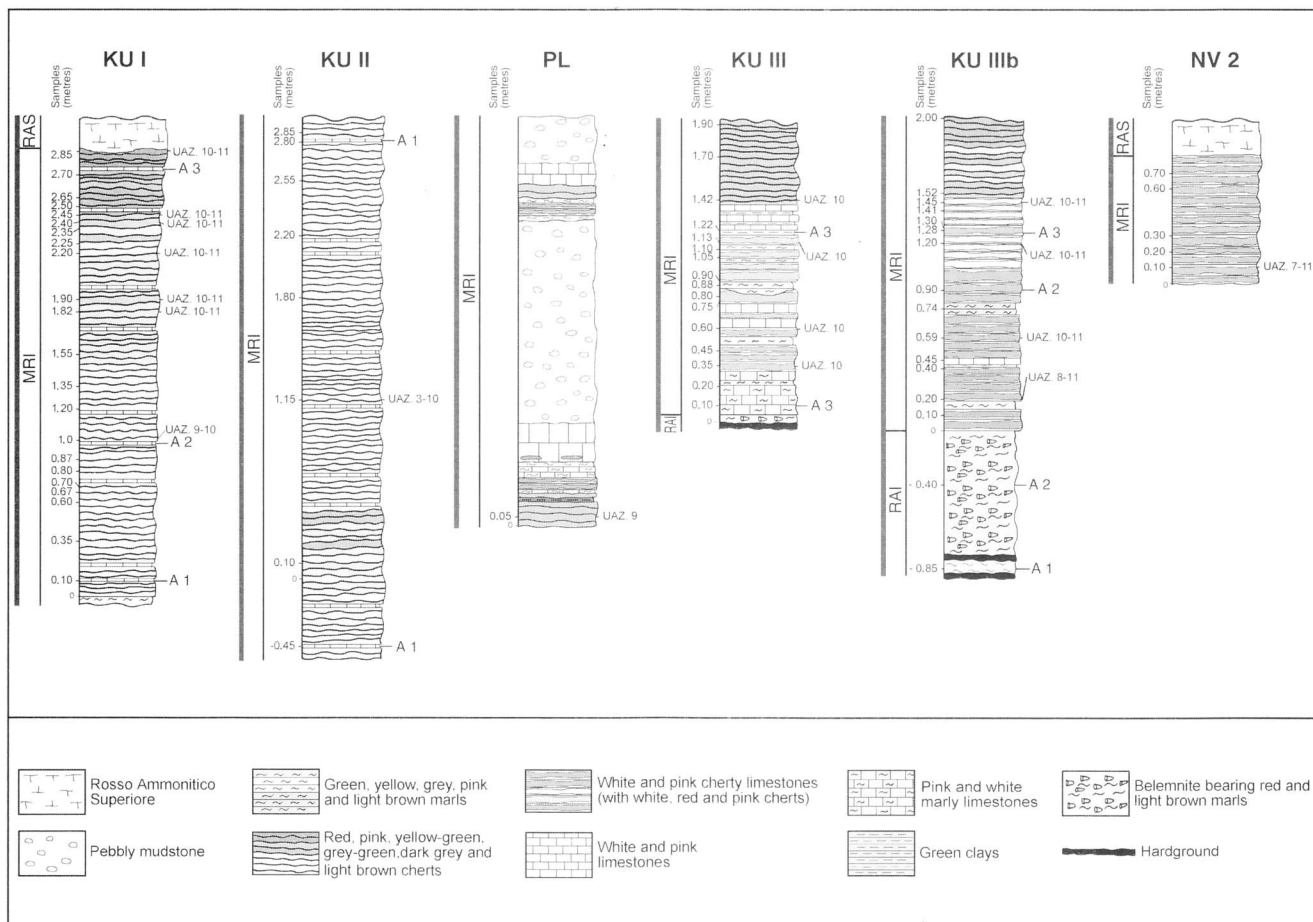


Fig. 4 - Lithological logs of the Monte Kumeta sections with the main biostratigraphical data. RAI=Rosso Ammonitico Inferiore; MRI=Membro Radiolaritico Intermedio; RAS=Rosso Ammonitico Superiore. UAZ.=Unitary Association Zones (Radiolarians); A=calcareous nanofossil assemblages. For location of sections see fig. 2.

of red cherty limestones (layers from 2 to 4 cm, with red chert), capped by the RAS beds.

Biostratigraphy

Radiolarians

Analyses of radiolarians have been performed on sixty-five samples. The radiolarians have been extracted from the siliceous samples with hydrofluoric acid at different concentrations (about 300 residues have been examined at the stereomicroscope) with the method proposed by Dumitrica (1970), Pessagno & Newport (1972), Baumgartner et al. (1981), De Wever (1982). The radiolarian bearing samples were collected in several sections of Monte Kumeta, but only a few of them contain radiolarians well preserved enough to obtain precise age determinations (Pl.1). The radiolarian zonation based on Unitary Association Zones (UAZ.) proposed by Baumgartner et al. (1995) is adopted herein.

A list of the most important taxa for the age determination is given in the following paragraphs.

In Tab. 1 the complete faunal assemblages from the

examined samples are shown and in Tab. 2 we report the age range of the most important radiolarian taxa.

KU I Section

Sample KU I 1.0: middle-late Oxfordian to late Oxfordian-early Kimmeridgian (UAZ. 9-10) based on the occurrence of *Emiluvia pentaporata* Steiger & Steiger and *Tritrabs casmaliaensis* (Pessagno).

Sample KU I 1.82: late Oxfordian-early Kimmeridgian to late Kimmeridgian-early Tithonian (UAZ. 10-11) based on the occurrence of *Emiluvia orea ultima* Baumgartner & Dumitrica, *Emiluvia pentaporata* Steiger & Steiger and *Triactoma blakei* (Pessagno).

Sample KU I 1.90: late Oxfordian-early Kimmeridgian to late Kimmeridgian-early Tithonian (UAZ. 10-11) based on the occurrence of *Emiluvia orea ultima* Baumgartner & Dumitrica and *Tetratrabs bulbosa* Baumgartner.

Sample KU I 2.20: late Oxfordian-early Kimmeridgian to late Kimmeridgian-early Tithonian (UAZ. 10-11) based on the occurrence of *Emiluvia orea ultima* Baumgartner & Dumitrica and *Triactoma foremanae* Muzavor.

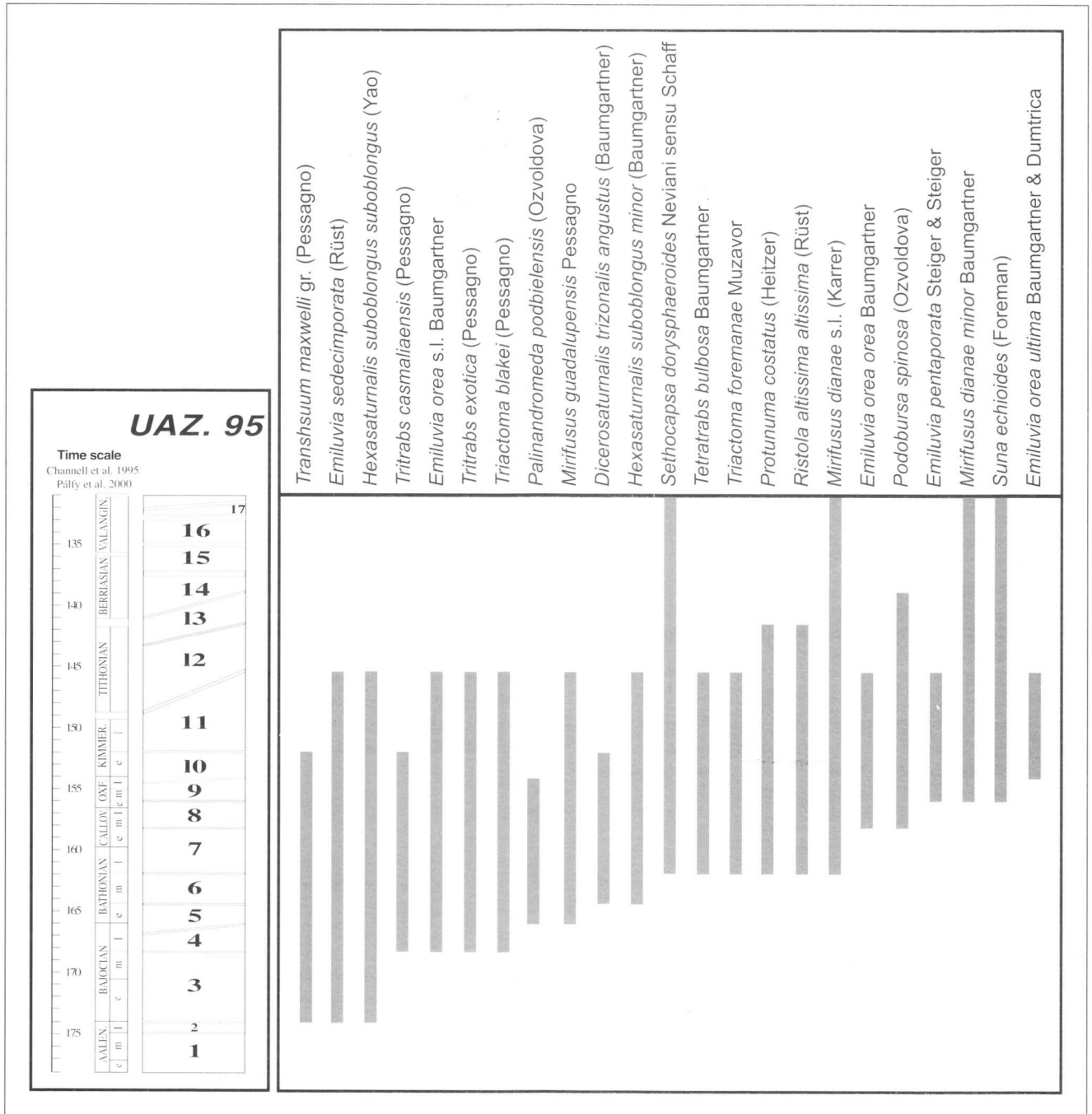
Sample KU I 2.40: late Oxfordian-early Kimmeridgian to late Kimmeridgian-early Tithonian (UAZ. 10-11) based on the occurrence of *Emiluvia orea ultima* Baumgartner & Dumitrica.

Sample KU I 2.45: middle Callovian-early Oxfordian to latest Tithonian (UAZ. 8-13) based on the occurrence of *Podobursa spinosa* (Ozoldova).

Sample KU I 2.85: late Oxfordian-early Kimmeridgian to late Kimmeridgian-early Tithonian (UAZ. 10-11) based on the occurrence

Sections		KU I							KU II	PL	KU III					KU IIIb					NV 2					
Taxa	Samples	1.0	1.82	1.90	2.20	2.40	2.45	2.70	2.85	1.15	0.05	0.35	0.60	1.10	1.13	1.42	0.20	0.45	0.59	1.20	1.45	0.10	0.20	0.60		
<i>Archaeodictyomitra</i> sp. cf. <i>A. minoensis</i> (Mizutani)																										
<i>Archaeodictyomitra</i> sp.																										
<i>Crucella</i> sp.																										
<i>Dicerosaturnalis trizonalis angustus</i> (Baumgartner)																										
<i>Dicerosaturnalis</i> sp.																										
<i>Emiluvia orea orea</i> Baumgartner																										
<i>Emiluvia orea ultima</i> Baumgartner & Dumitrica																										
<i>Emiluvia orea</i> s.l. Baumgartner																										
<i>Emiluvia pentaporata</i> Steiger & Steiger																										
<i>Emiluvia</i> sp. cf. <i>E. ordinaria</i> Ozvoldova																										
<i>Emiluvia</i> sp. cf. <i>E. orea ultima</i> Baumgartner & Dumitrica																										
<i>Emiluvia</i> sp. cf. <i>E. orea</i> s.l. Baumgartner																										
<i>Emiluvia</i> sp. cf. <i>E. pentaporata</i> Steiger & Steiger																										
<i>Emiluvia</i> sp. cf. <i>E. pessagnoi</i> s.l. Foreman																										
<i>Emiluvia</i> sp. cf. <i>E. salensis</i> Pessagno																										
<i>Emiluvia</i> sp.																										
<i>Hexasaturnalis suboblongus suboblongus</i> (Yao)																										
<i>Hexasaturnalis suboblongus minor</i> (Baumgartner)																										
<i>Hexasaturnalis</i> sp. cf. <i>H. suboblongus suboblongus</i> (Yao)																										
<i>Mirifusus diana minor</i> Baumgartner																										
<i>Mirifusus diana</i> s.l. (Karrer)																										
<i>Mirifusus guadalupensis</i> Pessagno																										
<i>Mirifusus</i> sp.																										
<i>Napora</i> sp. cf. <i>N. lospensis</i> Pessagno																										
<i>Palinandromeda podbielensis</i> (Ozvoldova)																										
<i>Paronaella</i> sp.																										
<i>Podobursa spinosa</i> (Ozvoldova)																										
<i>Podobursa triacantha</i> s.l. (Fischli)																										
<i>Podobursa</i> sp. cf. <i>P. polyacantha</i> (Fischli)																										
<i>Podobursa</i> sp. cf. <i>P. spinosa</i> (Ozvoldova)																										
<i>Podobursa</i> sp. cf. <i>P. triacantha</i> s.l. (Fischli)																										
<i>Podobursa</i> sp.																										
<i>Praeconsphaera sphaeroconus</i> (Rüst)																										
<i>Praeconsphaera</i> sp. cf. <i>P. sphaeroconus</i> (Rüst)																										
<i>Praeconsphaera</i> sp.																										
<i>Protunuma costatus</i> (Heitzer)																										
<i>Protunuma</i> sp. cf. <i>P. costatus</i> (Heitzer)																										
<i>Protunuma</i> sp.																										
<i>Ristola altissima altissima</i> (Rüst)																										
<i>Ristola</i> sp. cf. <i>R. altissima altissima</i> (Rüst)																										
<i>Sethocapsa dorysphaeroides</i> Neviani sensu Schaff																										
<i>Sethocapsa</i> sp.																										
<i>Suna echioides</i> (Foreman)																										
<i>Syringocapsa</i> sp.																										
<i>Tetratrabs bulbosa</i> Baumgartner																										
<i>Tetratrabs</i> sp. cf. <i>T. bulbosa</i> Baumgartner																										
<i>Tetratrabs</i> sp. cf. <i>T. zealis</i> (Ozvoldova)																										
<i>Tetratrabs</i> sp.																										
<i>Transhuum maxwelli</i> gr. (Pessagno)																										
<i>Triactoma blakei</i> (Pessagno)																										
<i>Triactoma foremanae</i> Muzavor																										
<i>Triactoma</i> sp. cf. <i>T. blakei</i> (Pessagno)																										
<i>Triactoma</i> sp. cf. <i>T. foremanae</i> Muzavor																										
<i>Triactoma</i> sp.																										
<i>Tritrabs casmaliensis</i> (Pessagno)																										
<i>Tritrabs exotica</i> (Pessagno)																										
<i>Tritrabs</i> sp. cf. <i>T. ewingi</i> s.l. (Pessagno)																										
<i>Tritrabs</i> sp. cf. <i>T. exotica</i> (Pessagno)																										
<i>Tritrabs</i> sp.																										
<i>Wrangellium</i> sp. cf. <i>W. brevicostatum</i> gr. (Ozvoldova)																										
<i>Wrangellium</i> sp.																										

Tab. 1 - Occurrence chart of the radiolarian taxa in the studied sections.



Tab. 2 - Range chart of the radiolarian taxa. Radiolarian zonation after Baumgartner et al. (1995). Range of *Hexasaturnalis suboblongus minor* after Dumitrica (pers. comm.) Time scale after Channell et al. (1995) and Pálffy et al. (2000).

of *Emiluvia orea ultima* Baumgartner & Dumitrica and *Tetratrabs bulbosa* Baumgartner.

We observed in the sample KU I 1.0, the coexistence of forms that should not be associated after the biozonation proposed by Baumgartner et al. (1995), such as *Emiluvia pentaporata* Steiger & Steiger (*Emiluvia bisellea* Danelian in Baumgartner et al. 1995 - UAZ. 11-11) and *Tritrabs casmaliensis* (Pessagno) (UAZ. 6-10). It is worth of note that *Emiluvia pentaporata* Steiger & Steiger was also found in a sample of Oxfordian age collected in the Carpathians (Dumitrica pers. comm.). We propose to indicate for *Emiluvia pentaporata* Steiger & Steiger a longer range (UAZ. 9-11).

KU II section

Sample KU II 1.15: early-middle Bajocian to late Oxfordian-

early Kimmeridgian (UAZ. 3-10) based on the occurrence of *Transsuum maxwelli* gr. (Pessagno).

KU IIIb Section

Sample KU IIIb 0.20: middle Callovian-early Oxfordian to late Kimmeridgian-early Tithonian (UAZ. 8-11) based on the occurrence of *Emiluvia orea orea* Baumgartner and *Podobursa spinosa* (Ozvoidova).

Sample KU IIIb 0.59: late Oxfordian-early Kimmeridgian to late Kimmeridgian-early Tithonian (UAZ. 10-11) based on the occurrence of *Emiluvia orea* s.l. Baumgartner, *Emiluvia orea ultima* Baumgartner & Dumitrica and *Tetratrabs bulbosa* Baumgartner.

Sample KU IIIb 1.20: late Oxfordian-early Kimmeridgian to late Kimmeridgian-early Tithonian (UAZ. 10-11) based on the occurrence of *Emiluvia orea ultima* Baumgartner & Dumitrica, *Emiluvia pentapo-*

rata Steiger & Steiger, *Tetrarabs bulbosa* Baumgartner and *Triactoma foremanae* Muzavor.

Sample KU IIIb 1.45: late Oxfordian-early Kimmeridgian to late Kimmeridgian-early Tithonian (UAZ. 10-11) based on the occurrence of *Emiluvia orea ultima* Baumgartner & Dumitrica and *Triactoma foremanae* Muzavor.

KU III Section

Sample KU III 0.35: late Oxfordian-early Kimmeridgian to late Kimmeridgian-early Tithonian (UAZ. 10-11) based on the occurrence of *Emiluvia orea* s.l. Baumgartner, *Emiluvia orea ultima* Baumgartner & Dumitrica and *Triactoma foremanae* Muzavor.

Sample KU III 0.60: late Oxfordian-early Kimmeridgian to late Kimmeridgian-early Tithonian (UAZ. 10-11) based on the occurrence of *Emiluvia orea ultima* Baumgartner & Dumitrica and *Emiluvia orea* s.l. Baumgartner.

Sample KU III 1.13: middle-late Oxfordian to late Kimmeridgian-early Tithonian (UAZ. 9-11) based on the occurrence of *Mirifusus diana minor* Baumgartner, *Mirifusus guadalupensis* Pessagno and *Triactoma foremanae* Muzavor.

Sample KU III 1.42: late Bathonian-early Callovian to late Oxfordian-early Kimmeridgian (UAZ. 7-10) based on the occurrence of *Dicerosaturnalis trizonalis angustus* (Baumgartner) and *Tetrarabs bulbosa* Baumgartner.

PL Section

Sample PL 0.05: middle-late Oxfordian (UAZ. 9) based on the occurrence of *Palinandromeda podbielensis* (Ozoldova) and *Suna echioides* (Foreman).

NV 2 Section

Sample NV 2 0.10: late Bathonian-early Callovian to late Kimmeridgian-early Tithonian (UAZ. 7-11) based on the occurrence of *Hexasaturnalis suboblongus minor* (Baumgartner), *Sethocapsa dorysphaeroides* Neviani sensu Schaff and *Tritrabs exotica* (Pessagno).

Calcareous nannofossils

A total of 80 samples were examined for calcareous nannofossil analysis using the standard techniques for smear slides preparation. The smear slides were observed under a light polarizing microscope, at 1000x magnification.

The analyzed lithologies are very variable, from calcareous to silty-calcareous with siliceous sediments. A mixture of calcareous and siliceous sediments is very common overall in the Monte Kumeta outcrops. Marly to calcareous-marly sediments are present in the Monte Kumeta, but generally a big amount of siliceous compounds are dispersed into the calcareous and marly sediments. Marls are the more favorable lithologies for calcareous nannofossil preservation because their shaly fraction develops thin films on the calcareous bodies that protect them from the aggressive diagenetic waters.

The marker events for the Middle - Late Jurassic, based on the FO (First Occurrence) and LO (Last Occurrence) of the members of the family Stephanolithaceae, are totally lacking. However, others accessory events can be usefully utilized.

The nannofossil zonation schemes utilized in this work are those of Mattioli & Erba (1999) for the Aalenian - Bathonian interval, and Bralower et al. (1989) for the Oxfordian - Tithonian interval.

Calcareous nannofossil assemblages

Three representative assemblages (A1, A2 and A3) were identified and utilized for the age determinations; for each section the assemblages are reported in the schematic columnar log (Fig. 4).

Assemblage 1 - is characterized by common *Watznaueria barnesae* (Black in Black & Barnes 1959) Perch-Nielsen, 1968, *Watznaueria contracta* (Bown & Cooper, 1989), Cobiachi, Erba & Pirini Radrizzani, 1992, *Watznaueria manivittae* Bukry, 1973d, *Watznaueria britannica* (Stradner, 1963) Reinhardt 1964, *Watznaueria fossacinta* (Black, 1971) Bown in Bown & Cooper 1989, *Cyclagelosphaera margerelii* Noël, 1965, *Triscutum* spp., *Lotharingius hauffii* Grün & Zweili in Grün et al. 1974, *Lotharingius crucentralis* (Medd, 1971) Grün & Zweili 1980 and *Schizosphaerella* spp. This assemblage is referable to lower-middle Bathonian based on the presence of *W. barnesae* and the absence of *Cyclagelosphaera wiedmannii* Reale & Monechi 1994; Mattioli & Erba (1999) reported the FO of *C. wiedmannii* as upper Bathonian. This assemblage is present at the base of the KU I, characterizes all the KU II section and the base of the KU III b section.

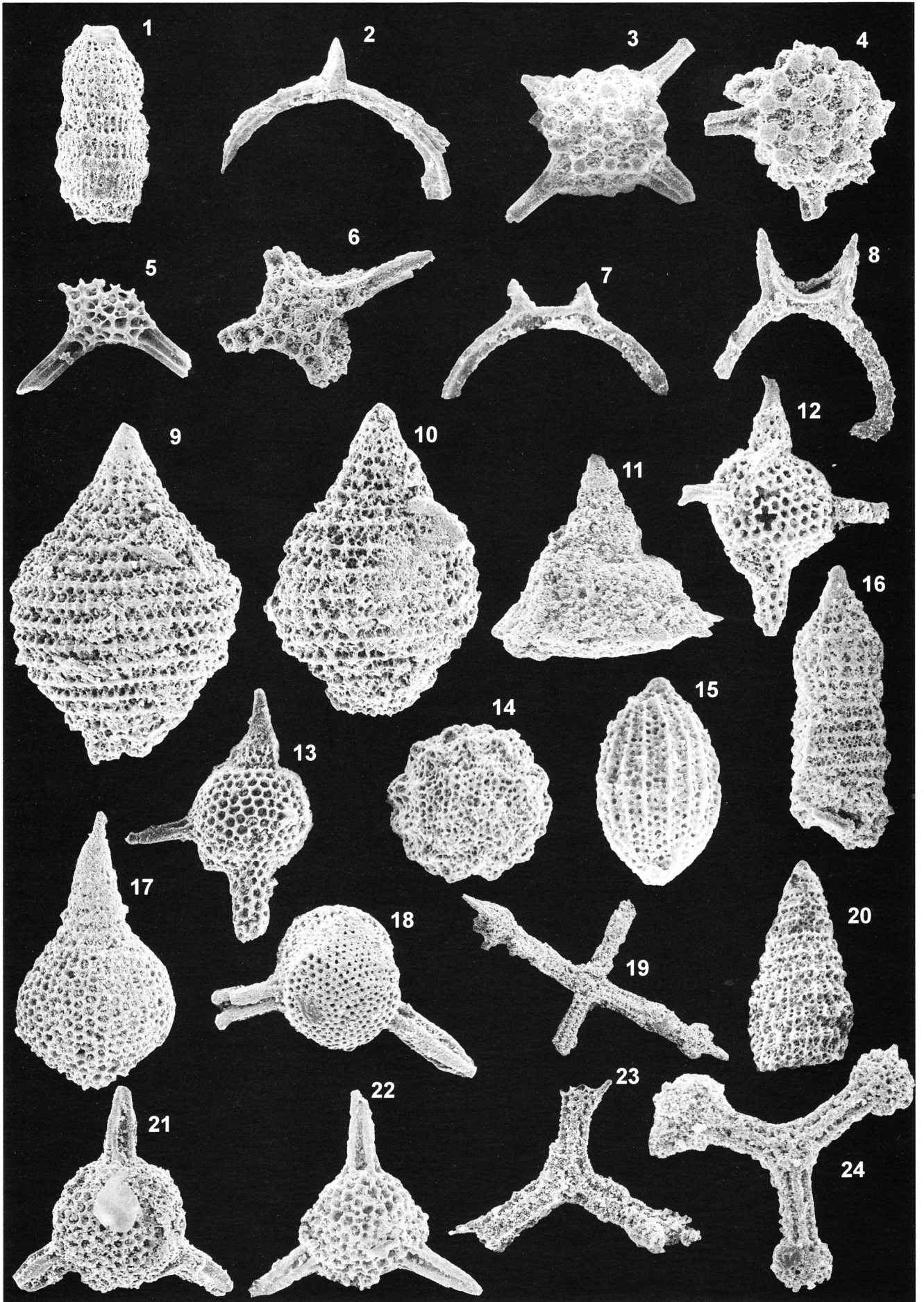
Assemblage 2 - is characterized by the presence of *C. wiedmannii* and the absence of *Schizosphaerella* spp. in assemblage. Moreover the presence of *L. crucentralis* and *L. hauffii*, old survivor taxa from the Pliensbachian assemblages, allows to infer the assemblage age. Bown (1998) reported the LOs of *L. crucentralis* and *L. hauffii* during the Oxfordian, while Bartolini et al. (1995) reported this event during lower Kimmeridgian. Consequently, this assemblage could be referred to the upper Bathonian - lower Kimmeridgian interval. Assemblage 2 is present in the middle portions of the KU I and KU IIIb sections.

Assemblage 3 - is characterized by *C. wiedmannii*, *W. barnesae*, *W. britannica*, *W. manivittae*, *W. contracta*, *C. margerelii*, *W. biporta* and the absence of species of the genus *Lotharingius*. Assemblage 3 is found at the top of KU I section, in all the KU III section and in the upper portion of KU IIIb section. This assemblage indicates an age not older than lower Kimmeridgian.

PLATE 1

Scanning electron microphotographs of radiolarians from the Membro Radiaratico Intermedio in the Monte Kumeta sections. For each figure the sample numbers and the magnification are indicated.

Fig. 1 - *Archaeodictyomitra* sp. cf. *A. minoensis* (Mizutani), KU I 2.70 (x150). Fig. 2 - *Dicerosaturnalis trizonalis angustus* (Baumgartner), KU III 1.42 (x130). Fig. 3 - *Emiluvia orea orea* Baumgartner, KU IIIb 0.20 (x100). Fig. 4 - *Emiluvia orea ultima* Baumgartner & Dumitrica, KU I 2.40 (x100). Fig. 5 - *Emiluvia pentaporata* Steiger & Steiger, KU I 1.0 (x100). Fig. 6 - *Emiluvia pentaporata* Steiger & Steiger, KU IIIb 1.20 (x100). Fig. 7 - *Hexasaturnalis suboblongus minor* (Baumgartner), KU IIIb 1.45 (x130). Fig. 8 - *Hexasaturnalis suboblongus suboblongus* (Yao), KU I 1.90 (x130). Fig. 9 - *Mirifusus diana minor* Baumgartner, KU II-Ib 1.45 (x100). Fig. 10 - *Mirifusus guadalupensis* Pessagno, KU III 1.13 (x100). Fig. 11 - *Palinandromeda podbielensis* (Ozoldova), PL 0.05 (x100). Fig. 12 - *Podobursa spinosa* (Ozoldova), KU IIIb 1.45 (x130). Fig. 13 - *Podobursa triacantha* s.l. (Fischli), KU IIIb 0.59 (x100). Fig. 14 - *Praeconosphaera sphaeroconus* (Rüst), KU IIIb 1.45 (x100). Fig. 15 - *Protunuma costatus* (Heitzer), KU IIIb 1.45 (x200). Fig. 16 - *Ristola altissima altissima* (Rüst), KU IIIb 1.45 (x100). Fig. 17 - *Sethocapsa dorysphaeroides* Neviani sensu Schaff, NV 2 0.10 (x100). Fig. 18 - *Suna echioides* (Foreman), PL 0.05 (x100). Fig. 19 - *Tetrarabs bulbosa* Baumgartner, KU I 2.85 (x50). Fig. 20 - *Transsuum maxwelli* gr. (Pessagno), KU II 1.15 (x130). Fig. 21 - *Triactoma blakei* (Pessagno), KU I 1.82 (x100). Fig. 22 - *Triactoma foremanae* Muzavor, KU III 1.13 (x100). Fig. 23 - *Tritrabs casmaliaensis* (Pessagno), KU I 1.0 (x100). Fig. 24 - *Tritrabs exotica* (Pessagno), NV 2 0.10 (x100).



SECTION		KU I	KU II	PL	KU III	KU IIIB	NV 2
AGE							
Kimmeridgian	L	RAS					RAS
	E				MRI	MRI	
Oxfordian	L			MRI	GAP		
	M				RAI		
	E					RAI	MRI
Callovian	L	MRI					
	M						
	E					GAP	
Bathonian	L						
	M		MRI			RAI	?
	E						

Fig. 5 - Chrono-correlation between the lithostratigraphic units in the examined sections.

Discussion and conclusions

The Monte Kumeta area represents an example of a stepped pelagic escarpment adjacent to a Jurassic intra-basinal high, which formed in Early Jurassic times by extensional tectonics (Mariotti et al. 2001; Di Stefano et al. 2002a). The dip of the paleoescarpment was to the NE-SW and it is shown now by the NE-SW thickening of the successions. Near the top of the Monte Kumeta the carbonate and siliceous deposits pinch out and only the Inici Fm. crops out. The lack of a condensed pelagic succession conformably lying on the Inici Fm. and volumes of resedimented material imply that much of the original depositional system is not preserved (Marino et al. 2002).

The thickness of the Membro Radiolaritico Intermedio is variable as well as its lithology, state of preservation and frequency of radiolarians and calcareous nanofossils. Several samples were collected in the sections of Monte Kumeta but only a few of them were rich enough in radiolarians and calcareous nanofossils to be useful.

The most important results of this integrated study are as follows (Fig. 5):

Section KUI, the base is referable to lower-middle Bathonian using the calcareous nanofossil data (Assemblage 1). The co-occurrence of the calcareous nanofossil Assemblage 2 and of the radiolarian assemblage referable to the UAZ. 9-10 could be indicative of middle Oxfordian - lower Kimmeridgian. At the top of the section the presence of the calcareous nanofossil Assemblage 3 and radiolarian assemblage referable to the UAZ. 10-11 allows the identification of an age not older than early Kimmeridgian. We observed, in the sample KU I 1.0, the coexistence of *Emiluvia pentaporata* Steiger & Steiger (*Emiluvia bisellea* Danelian in Baumgartner et al., 1995 - UAZ. 11-11) and *Tritrabs casmaliaensis* (Pessagno) (UAZ. 6-10). We propose, in according to these data and the radiolarian data from a section in the Carpathians (Dumitrica pers. com.), to indicate for *Emiluvia pentaporata* Steiger & Steiger a longer range (UAZ. 9-11).

The **KU II section** is all referable to lower-middle Bathonian based on the presence of the calcareous nanofossil Assemblage 1 in agreement with data from the radiolarian assemblage (UAZ. 3-10).

In **section PL** it has been possible to give, with the radiolarian biostratigraphy, an age limit to the emplace-

ment of a pebbly mudstone in the Membro Radiolaritico Intermedio. In fact the radiolarian assemblage of sample PL 0.05, collected at the base of the section, indicates a middle-late Oxfordian age (UAZ. 9). Hence the emplacement of the pebbly mudstone could be referable to the late Oxfordian or younger.

In **section KU III** the calcareous nannofossil assemblage (Assemblage 3) indicates an age not older than early Kimmeridgian according to the radiolarian data (UAZ. 10). The presence at the base of the section of a Belemnite level (RAId) referable to late Callovian - middle Oxfordian (Mariotti 2002) could indicate a stratigraphic discontinuity probably referable to a sedimentary hiatus.

The base of the KU IIIb section is referable to the lower-middle Bathonian based on the presence of the calcareous nannofossil Assemblage 1. The occurrence of the calcareous nannofossil Assemblage 2 within the Belemnite level indicates a late Bathonian - early Kimmeridgian age. In the upper part of the section the finding of the calcareous nannofossil Assemblage 3 and of the radiolarian assemblage referable to UAZ. 10-11 allows to identify an age not older than early Kimmeridgian. At the base of the section the presence of the calcareous nannofossil Assemblage 1 proves the occurrence of a sedimentary gap from late Bathonian to early Callovian.

At the base of the **section NV 2** the radiolarian assemblage referable to UAZ. 7-11 is present. The scarce preservation of radiolarians does not permit to give an exact age to the base of the MRI in this section.

On the basis of these biostratigraphic data the chronostratigraphical range of the Membro Radiolaritico Intermedio could be considered as lower-middle Batho-

nian - lower Kimmeridgian. To obtain this age it was not sufficient to consider only the radiolarian and calcareous nannofossils data, we needed also to take into consideration biochronological data deriving from fossils present in the overlying unit. In fact the age of the ammonites collected in the Rosso Ammonitico Superiore is referable to late Kimmeridgian. Moreover this study shows that the age of Membro Radiolaritico Intermedio is variable depending on the different locations along the Monte Kumeta palaeoescarpment. In particular the age of the more distal sections span from early-middle Bathonian to the early Kimmeridgian while the proximal sections show ages referable to late Oxfordian - early Kimmeridgian (Fig. 5)

This age variation proves the presence of heteropy between the Membro Radiolaritico Intermedio and the Rosso Ammonitico Inferiore. Moreover, several local gaps occur in the Membro Radiolaritico Intermedio and they are restricted to late Bathonian - early Callovian and to late Oxfordian testifying times of more intense tectonic activity along the palaeoescarpment.

Acknowledgments. We thank U. Nicosia (Roma) for stimulating discussion. Careful reviews by B. Treves (Firenze) were very much appreciated. We also wish to thank P. Di Stefano (Palermo) and P. Dumitrica (Lausanne) for the critical revision of the manuscript.

This research was supported by research project MURST-COFIN 1999, 2001 (G. Parisi, University of Perugia); research project of University of Florence 2000, 2001 (60%; G. Principi) and by C.N.R. "Istituto di Geoscienze e Georisorse, Sezione di Firenze".

Radiolarian micrographs were taken by M. Ulivi, with a Philips 515 SEM of the MEMA, Dipartimento di Scienze della Terra, University of Florence and by S. Lazzeri, with a Philips XL20 SEM, of the Istituto per la Ricerca del Legno, C.N.R., Florence.

REFERENCES

- Abate B., Catalano R., D'Argenio B., Di Stefano P., Lo Cicero G., Vitale F., Agate M., Infuso S., Milia A., Nigro F. & Sulli A. (1990) - Jurassic to Tertiary sedimentary evolution of the Trapanese and Saccense Domains. Jurassic to Early Cretaceous transtensional tectonics versus Late Cretaceous-Eocene inversion. In: Catalano R. & D'Argenio B. (eds.): Hammering a seismic section, field trip in Western Sicily, Guide Book: 35-54. Dip. Geologia e Geodesia, Palermo.
- Baumgartner P. O., Björklund K. R., Caulet J. P., De Wever P., Kellogg D., Labracherie M., Nakaseko K., Nishimura A., Schaff A., Schmidt-Effing R. & Yao A. (1981) - *EuroRad II, 1980 - Second European meeting of radiolarian paleontologists: current research on Cenozoic and Mesozoic radiolarians*. *Ecl. geol. Helv.*, 74 (3): 1027-1061, Basel.
- Baumgartner P.O., Bartolini A.C., Carter E.S., Conti M., Cortese G., Danelian T., De Wever P., Dumitrica P., Dumitrica-Jud R., Gorican S., Guex J., Hull D.M., Kito N., Marcucci M., Matsuoka A., Murchey B., O'Dogherty L., Savary J., Vishnevskaya V., Widz D. & Yao A. (1995) - Middle Jurassic to Early Cretaceous Radiolarian biochronology of Tethys based on Unitary Associations. In: Baumgartner P.O. et al., (eds.) Middle Jurassic to Lower Cretaceous Radiolaria of Tethys: occurrences, systematics, biochronology. *Mém. Géol. Lausanne*, 23: 1013-1048, Lausanne.
- Bralower T.J., Monechi S. & Thierstein H. (1989) - Calcareous Nannofossil Zonation of the Jurassic-Cretaceous boundary interval and correlations with the Geomagnetic Polarity Timescale. *Mar. Micropal.*, 14: 153-235, Amsterdam.
- Caflich L. (1966). La Geologia dei Monti di Palermo. *Riv. Ital. Paleont. Strat. Mem.*, 12: 1-108, Milano.
- Catalano R. & D'Argenio B. (1982) - Schema geologico della Sicilia. In: Catalano R. & D'Argenio B. (eds.), Guida alla Geologia della Sicilia Occidentale. Soc. Geol. It., Guide Geologiche Regionali, 9-41, S.T. ASS., Palermo.

- Channel J.E.T., Erba E., Nakanishi M. & Tamaki K. (1995) - Late Jurassic-Early Cretaceous time scale and oceanic magnetic anomaly block model. In: *Geochronology, Time Scales and Global Stratigraphic Correlation. SEPM, Sp. Publ.*, 54: 51-63, Albuquerque.
- De Wever P. (1982) - Radiolaires du Trias et du Lias de la Téthys (Systématique, Stratigraphie). *Soc. Géol. Nord*, 7: 1-600, Villeneuve D'Ascq.
- Di Stefano P. & Mindszenty A. (2000) - Fe-Mn-encrusted "Kamenitza" and associated features in the Jurassic of Monte Kumeta (Sicily): subaerial and/or submarine dissolution? *Sedimentary Geology*, 132: 37-68, Amsterdam.
- Di Stefano P., Gálaczi A., Mallarino G., Mindszenty A. & Vörös A. (2002a). Birth and early evolution of a Jurassic escarpment: Monte Kumeta, Western Sicily. *Facies*, 46: 273-298, Erlangen.
- Di Stefano P., Gálaczi A., Mallarino G., Mindszenty A. & Vörös A. (2002b). Birth and dynamics of a Jurassic submarine escarpment at Monte Kumeta. In: Santantonio M. (ed.) *General Field Trip Guidebook, 6th International Symposium on the Jurassic System*: 198-208, GEDA Torino.
- Dumitrica P. (1970). Cryptocephalic and cryptothoracic Nassellaria in some Mesozoic deposits of Romania. *Rev. Roum. Géol. Géophys. Géogr. sér. Géol.*, 14 (1): 45-124, Bucarest.
- Marino M., Nicosia U. & Santantonio M. (2002) - Late Jurassic evolution of the submarine escarpment at Monte Kumeta - an introduction. In: Santantonio M. (ed.) *General Field Trip Guidebook, 6th International Symposium on the Jurassic System*: 209-219, GEDA, Torino.
- Mariotti N., Baldanza A., Chiari M., Di Stefano P., Mallarino G., Marino M., Muraro C., Nicosia U., Parisi G., Petti F. M. & Santantonio M. (2001). La scarpata di M. Kumeta (Sicilia) nel Giurassico superiore. *Atti 3^o Convegno FIST*, Chieti: 216-218, Media Print, Livorno.
- Mariotti N. (2002) - Upper Callovian - Middle Oxfordian belemnite assemblage from Monte Kumeta (Jurassic of western Sicily, Italy). *Boll. Soc. Paleont. It.*, 41 (1): 13-35, Modena.
- Masclé G. (1979) - Etude géologique des Monts Sicani. *Mem. Riv. It. Paleont. Strat. Mem.*, 16: 1-431, Milano.
- Mattioli E. & Erba E. (1999) - Synthesis of calcareous nanofossil events in Tethyan Lower and Middle Jurassic successions. *Riv. Ital. Paleont. Strat.*, 105: 343-376, Milano.
- Pálffy J., Smith P.L. & Mortensen J.K. (2000). A U-PB and ⁴⁰AR/³⁹AR time scale for the Jurassic. *Can. J. Earth Sci.*, 37: 1-23, Ottawa.
- Pessagno E. A. & Newport L. A. (1972) - A technique for extracting Radiolaria from radiolarian chert. *Micropaleontology*, 18 (2): 231-234, New York.
- Wendt J. (1963) - Stratigraphisch-paläontologische Untersuchungen im Dogger Westsiziliens. *Boll. Soc. Paleont. It.*, 2 (1): 57-145, Modena.
- Wendt J. (1969) - Die stratigraphisch-paläontologische Entwicklung des Jura in Westsizilien. *Geol. Rundsch.*, 58 (3): 735-755, Berlin.